OPTICAL PROPERTIES OF THE SEMICONDUCTING "METAL-LIKE" COMPLEX (NMe₃H) (I) (TCNQ)

D.B. Tanner and J.E. Deis

Department of Physics, The Ohio State University, Columbus, OH 43210, U.S.A.

and

A.J. Epstein and J.S. Miller*

Xerox Webster Research Center, Rochester, NY 14644, U.S.A.

We present the results of a study of the room temperature polarized reflectance between 2.5 meV and 3.8 eV of $(NMe_3H)(I)(TCNQ)$ single crystals. The reflectance found with the electric field parallel to the stacking axis is fit with a Drude–Lorentz model and analyzed using Kramers–Kronig transforms to give the response functions $\sigma_1(\omega)$ and $\epsilon_1(\omega)$. The results confirm the model of semiconducting behavior despite a "metal-like" d.c. electrical conductivity at room temperature.

THE STUDY of linear chain organic [1] and inorganic [2] anisotropic compounds has emphasized those system systems with high "metal-like" conductivity, and the competing models to explain this behavior. Recently, Cougrand et al. [3] have reported that the tetracyanoquinodimethane (TCNQ) oxidation of trimethyl-ammonium iodide $(NMe_3H)^+(I)^-(Me=CH_3)$ leads to a novel ternary component material of $(NMe_3H)(I)(TCNQ)$ stoichiometry with one donor and two different segregated acceptor chains, only one of which, TCNQ, is likely to be conducting. In this paper we present the results of a study of the room temperature polarized reflectance, from the far infrared to the near ultraviolet, of $(NMe_3H)(I)(TCQN)$ which confirms that it is a semiconductor despite its "metal-like" conductivity.

The structure of this system is monoclinic with the TCNQ chains and the iodine chains parallel to the b-axis [3]. The long axes of the TCNQ molecules are all parallel to each other and are perpendicular to the a-axis. In a diffuse X-ray investigation, Delhaes et al. [4] reported a one-dimensional superlattice ascribed to a periodic distortion (period 3b) on the iodine chain. The results of Abkowtiz et al. [5, 6] indicate that the composition is best described as $(NMe_3H)^+(I_3^-)_{1/3}$-$(TCNQ)^{2/3-}$ with a 1/3 filled band on the TCNQ chains in a one-electron picture. The room temperature d.c. electrical conductivity is $\sigma_{RT} \simeq 20 \ (\Omega\text{-cm})^{-1}$, with "metal-like" behavior between 300 and 240 K at which latter temperature $(T = T_M)$ it achieves its maximum value, $\sigma = 1.08\sigma_{RT}$ [7].

Recently, Epstein et al. [8–10] have proposed a model for conduction in many TCNQ salts with "metal-like" behavior $(d\sigma/dT < 0)$ which postulates a semiconducting state at all temperatures. For $T > T_M$, σ is dominated by a strongly temperature dependent mobility determined in large part by interactions between the conduction electrons and molecular vibrations. For $T < T_M$, $\sigma(T)$ is dominated by the thermal activation of carriers across the gap. The model requires significant coupling of the conduction electrons to molecular vibration modes of TCNQ, an effect which has been observed in (triethylammonium)(TCNQ) [11] and in (K)(TCNQ) [12]. The model predicts the existence of a semiconducting energy gap for $(NMe_3H)(I)(TCNQ)$ at 300 K of ~ 0.14 eV.

Polarized reflectance measurements have been made on room temperature lustrous metallic green specimens using conventional techniques. Figure 1 shows the reflectance, R, of $(NMe_3H)(I)(TCNQ)$ for three mutually perpendicular frequency independent extinction directions of the incident electric field. The measured R for $E \parallel b$ (the chain direction) was essentially the same for the two faces studied, as indeed it should be.

For $E \parallel a$ polarization, R is nearly flat. The molecular vibrational modes (e.g. C≡N at 2180 and 2220 cm^{-1}) are quite weak. The electric field is nearly perpendicular to the TCNQ molecule long axis, so this structure, as well as the C–H feature at 3020 cm^{-1} may be due to the $(NMe_3H)^+$ ion. For $E \parallel c^*$, R is slightly larger than $E \parallel a$ and a strong peak is seen at 2159 cm^{-1} in the C≡N stretching region. The c^* direction is nearly parallel to the TCNQ molecule long axis.

In the chain direction, $E \parallel b$, a strong peak in the visible (not shown, see [6]) is responsible for the green color. As is characteristic of many TCNQ salts [11–15], for $E \parallel b$ there is a weak structure in the near infrared

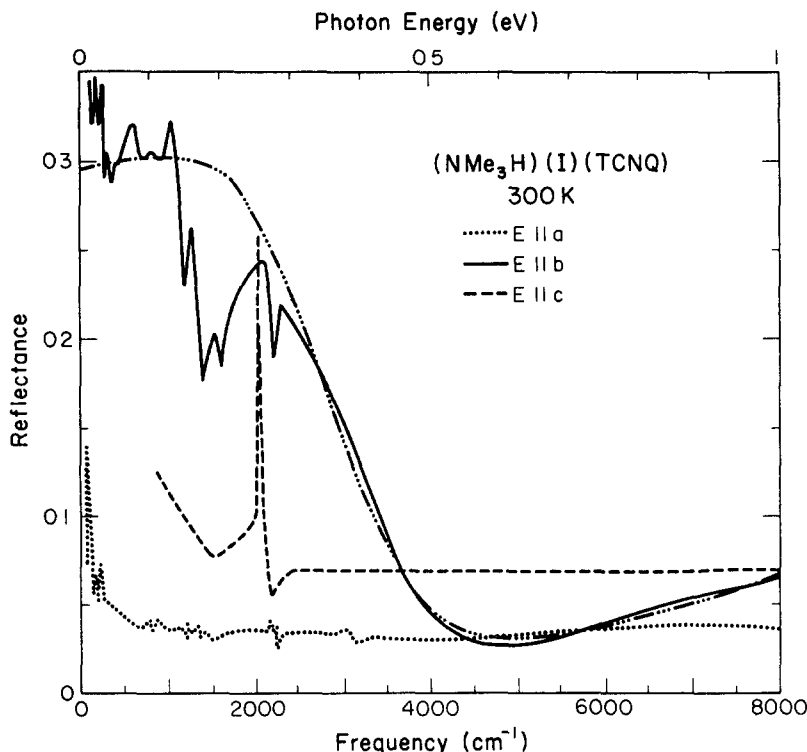* Current address: Occidental Research Center, Irvine, CA 92713, U.S.A.

Fig. 1. Polarized reflectance measurements over 0.0025–1 eV, of (NMe₃H) (I) (TCNQ) for three directions. The dash-dot curve is from a fit to the **E** || **b** data with a Drude–Lorentz dielectric function.

including a minimum at $4820\,\mathrm{cm}^{-1}$, and a broad reflectance maximum. Below $150\,\mathrm{cm}^{-1}$ the reflectance rises rapidly, reaching nearly unity at $20\,\mathrm{cm}^{-1}$. Between 1000 and $2300\,\mathrm{cm}^{-1}$ there are four clear minima, associated with symmetric stretching modes of the TCNQ ion [11, 12, 16].

A least squares fit to R for **E** || **b** was made for reflectance calculated from a Drude–Lorentz dielectric function of the form.

$$\epsilon(\omega) = \frac{\omega_p^2}{\omega_g^2 - \omega^2 - i\omega/\tau} + \frac{\omega_L^2}{\omega_0^2 - \omega^2 - i\omega\Gamma} + \epsilon_\infty.$$
(1)

The first term in equation (1) describes the reflectance maximum below $4800\,\mathrm{cm}^{-1}$, the second term includes the weak structure around $10\,000\,\mathrm{cm}^{-1}$, and the third term is the contribution of all higher frequency contributions to the static dielectric constant. The fit was made to the data between 2400 and $8000\,\mathrm{cm}^{-1}$ and the best results were obtained with the following parameters: strength of the first transition, $\omega_p = 0.66\,\mathrm{eV}$, center frequency, $\omega_g = 0.22\,\mathrm{eV}$, and relaxation rate, $1/\tau = 0.32\,\mathrm{eV}$. For the second transition, $\omega_L = 0.62\,\mathrm{eV}$, $\omega_0 = 1.2\,\mathrm{eV}$, and $\Gamma = 0.56\,\mathrm{eV}$. The high frequency dielectric constant is $\epsilon_\infty = 2.65$. If $\omega_g = 0$, equation (1) describes a metal. Fits to the data with a metallic dielectric function gave relatively poor results.

Because of the wide frequency range studied, a Kramer–Kronig integral of the reflectance should yield accurate values for the phase shift in the center of the experimental region. The data were extrapolated above the highest frequency point as $1/\omega^2$ up to $200\,000\,\mathrm{cm}^{-1}$, simulating in an average way interband transitions, and as $1/\omega^4$ above $200\,000\,\mathrm{cm}^{-1}$, as appropriate for free electron behaviour. Constant reflectance was assumed below the lowest data point. Neither the structure in the optical constants nor their magnitudes below $4000\,\mathrm{cm}^{-1}$ were changed by any extrapolation procedure tried.

The optical constants for 0–$8000\,\mathrm{cm}^{-1}$ (0–1 eV) are shown in Figs. 2 and 3. Figure 2 gives the frequency dependent conductivity, $\sigma_1(\omega)$ and Fig. 3 the real part of the dielectric function, $\epsilon_1(\omega)$. Below $200\,\mathrm{cm}^{-1}$ the average value of the conductivity is $\sigma_1 = 19 \pm 1$ $(\Omega\text{-cm})^{-1}$, in excellent agreement with the d.c. value of $20\,(\Omega\text{-cm})^{-1}$ [5–7]. (NMe₃H) (I) (TCNQ) is the first conducting TCNQ system in which there is agreement between the d.c. and far infrared conductivities! In (TTF) (TCNQ), for example [13,14], the far infrared conductivity is an order of magnitude *smaller* than the d.c. conductivity. There is a strong peak in $\sigma_1(\omega)$ centered near $\omega_g = 1770\,\mathrm{cm}^{-1}$ (0 22 eV). The full width at half maximum observed in Fig. 2 is approximately equal to the relaxation rate obtained from the
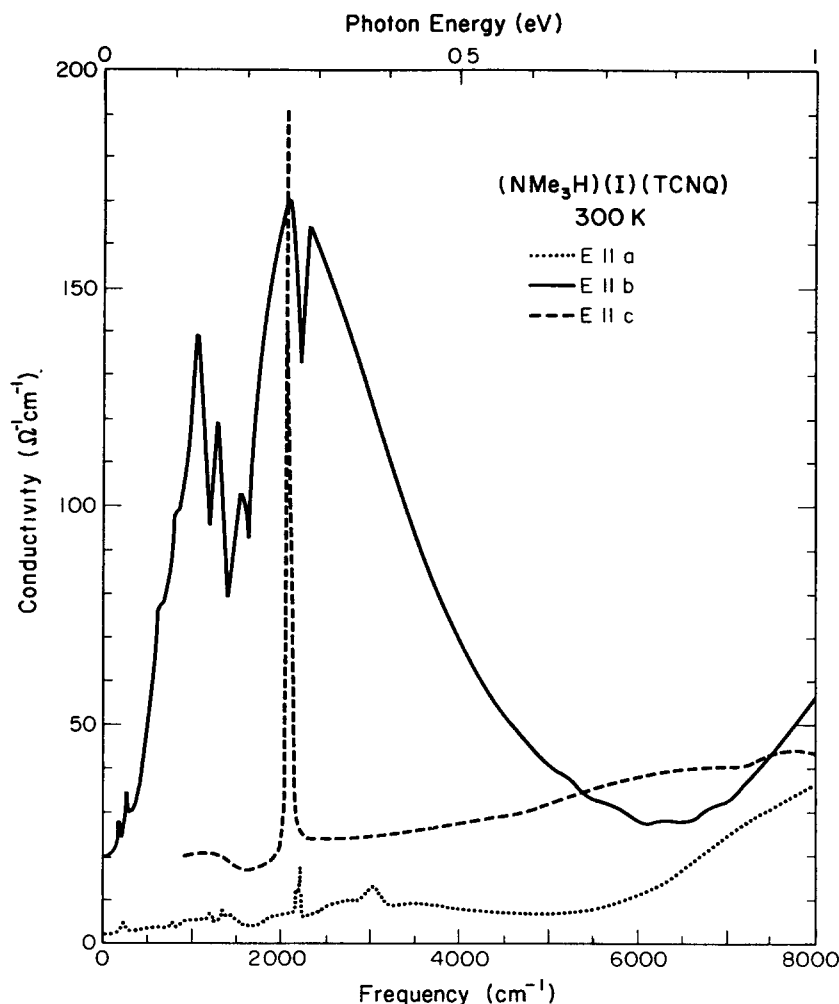
Fig. 2. Frequency dependent conductivity, determined by Kramers–Kronig analysis of the reflectance of (NMe₃H) (I) (TCNQ). The d.c. conductivity in $\sigma_{RT} \sim 20\ (\Omega\text{-cm})^{-1}$.

fit above 0.32 eV. The maximum value of the conductivity is 180 $(\Omega\text{-cm})^{-1}$ as expected from the Drude–Lorentz parameters, $\omega_p^2 \tau/4\pi$. Not shown in Fig. 2 is a strong conductivity maximum in the visible which reaches 1200 $(\Omega\text{-cm})^{-1}$ at 17,800 cm^{-1} (2.2 eV).

The dielectric function is negative below 40 cm^{-1}, characteristic of free carriers, and has a maximum of 10 in the far infrared. This value is comparable to the static value calculated from equation (1), $\epsilon_1(0) = 12$, but is considerably lower than the measured [6] microwave value at 4.2 K of $\epsilon_1 = 30$. The transition in the infrared is not quite strong enough to drive $\epsilon_1(\omega)$ negative between ω_g and ω_p, in part because of the relatively large value of ϵ_∞. The transition in the visible *is* sufficiently strong; $\epsilon_1(\omega)$ is negative between 19,000 cm^{-1} (2.4 eV) and 21,700 cm^{-1} (2.7 eV).

The implications of both the fit to the reflectance and the Kramers–Kronig analysis is that there is an energy gap in the system at room temperature even

though the dc conductivity is appreciable. The Drude–Lorentz dielectric function probably overestimates the gap. The conductivity reaches half of its maximum value at 800 cm^{-1} (0.10 eV) while about 1/8 of the interband oscillator strength is used up by 1100 cm^{-1} (0.14 eV). Either of these criteria might be reasonably used to define the edge of a rather smeared band gap. A gap of 0.10–0.14 eV is both in agreement with, and experimental evidence for, an analysis within the d.c. conductivity model [7–10] described above $(E_g \sim 0.14\,\text{eV at 300 K})$ [7]. The conductivity for $\omega < E_g$ is then due to carriers thermally excited across the gap. These "free carriers" in turn drive the dielectric function negative below 40 cm^{-1}. The gap at room temperature may arise from a periodic potential on the TCNQ chains induced by the observed [4] distortion on the iodine chain.

The effective number of electrons participating in transitions for energies less than $\hbar\omega$ is given by
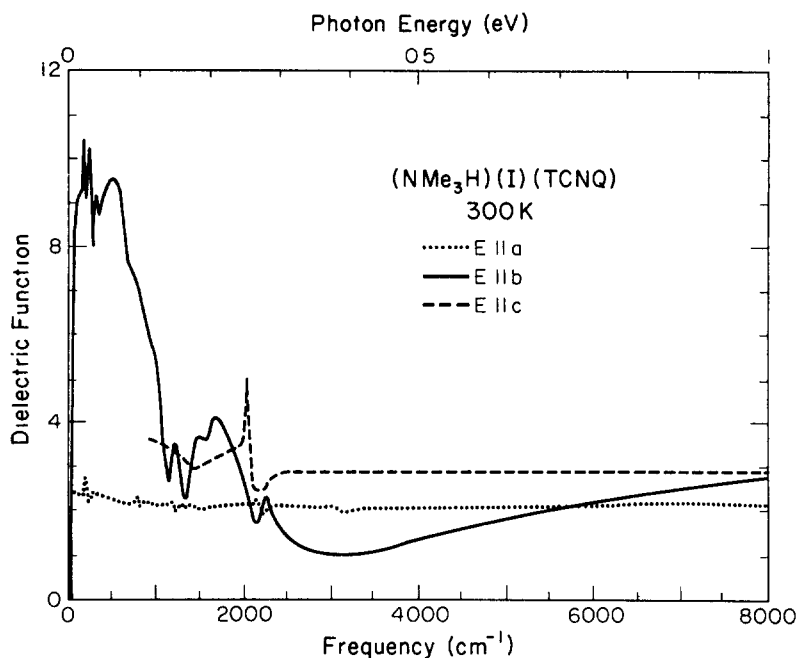
Photon Energy (eV)

Fig. 3. Real part of the dielectric function, determined by Kramers—Kronig analysis of the reflectance.
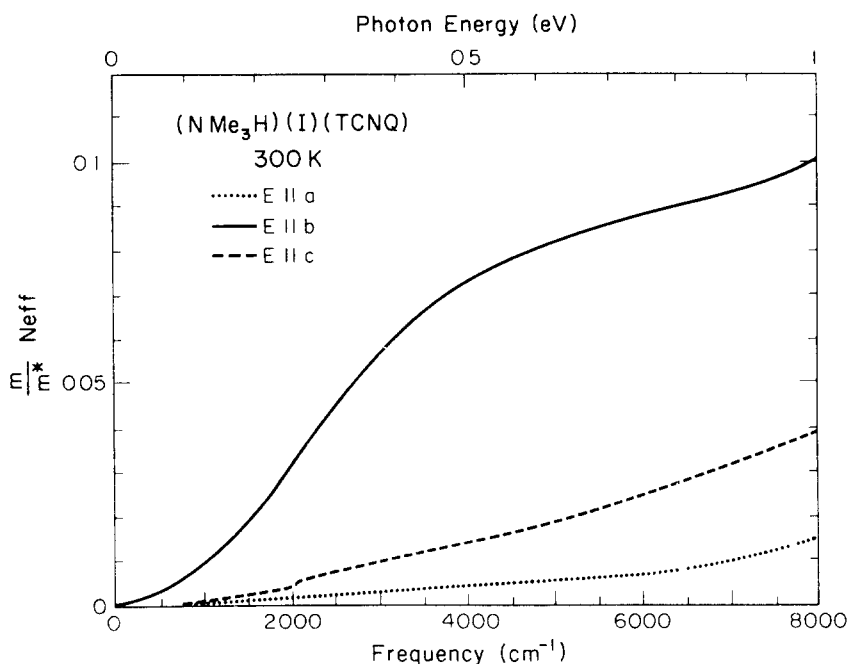
Photon Energy (eV)

Fig. 4. The effective number of electrons, determined by integration of the Kramers—Kronig derived conductivity.

$$\frac{m}{m^*} N_{\text{eff}}(\omega) = \frac{m V_m}{4\pi e^2} \int_0^\omega \sigma_1(\omega') \, d\omega' \qquad (2)$$

where m^* is the effective (band) mass of the carriers, m is the free electron mass, e the electronic charge, and V_m is the volume per molecule. From X-ray data [3, 5], $V_m = 410 \, \text{Å}$ [3]. For E ∥ b, $(m/m^*)N_{\text{eff}}$ increases rapidly at first and then begins to level off at a value near 0.1. It rises rapidly above 1 eV, reaching 1.5 at

3.1 eV. The function rises much more slowly and smoothly for the other two polarizations, see Fig. 4

The plateau value of $(m/m^*)N_{\text{eff}} = 0.1$ and the assumption of $N_{\text{eff}} = 0.67$, gives $m^* = 6.7m$. A similar effective mass is found from the plasma frequency, $\omega_p = (4\pi n e^2/m^*)^{1/2}$ where n is the number of conduction electrons per unit volume. When the plasma frequency obtained in the least squares fit, $\omega_p = 5290 \, \text{cm}^{-1}$ (0.66 eV), is substituted, we find, with

$N_{eff} = 0.67, m^* = 5.2m$.

The TCNQ salts form a unique system for the study of the electron–phonon interaction which has been investigated recently both experimentally [11, 12] and theoretically [16, 17]. The conduction electrons interact with the totally symmetric molecular vibrations of the TCNQ ion. Because the electrons are constrained in these quasi-1-D systems to move in the chain direction, the effect is observed when the electric field is polarized along the chain. When the electronic absorption overlaps the phonon frequencies, the interaction gives rise to minima or "antiresonances" in the conductivity of reflectance. This effect is readily observed in (NMe₃H)-(I) (TCNQ). In particular there are four distinct antiresonances in $\sigma_1(\omega)$, Fig. 2, at 1190, 1390, 1620 and 2208 cm⁻¹, as well as shoulders at lower frequencies. A detailed analysis is in progress.

REFERENCES

1. Proc. of the New York Academy of Sciences Conference on 'Synthesis and Properties of Low-Dimensional Materials' (Edited by J.S. Miller & A.J. Epstein), *Ann. N. Y. Acad. Sci.* **313** (1978).

2. J.S. Miller & A.J. Epstein, *Prog. Inorg. Chem.* **20**, 1 (1976).

3. A. Cougrand, S. Flandrois, P. Delhaes, P. Dupuis, D. Chasseau, J. Gaultier & J.L. Miane, *Mol. Cryst. Liq. Cryst.* **32**, 165 (1976).

4. P. Delhaes, A. Cougrand, S. Flandrois, D. Chasseau, J. Gaultier, C. Hauw & P. Dupuis, *Lecture Notes in Physics* **65**, 493 (1977).

5. M.A. Abkowitz, A.J. Epstein, C.H. Griffiths, J.S. Miller & M.L. Slade, *J. Am. Chem. Soc.* **99**, 5304 (1977).

6. M.A. Abkowitz, J.W. Brill, P.M. Chaikin, A.J. Epstein, M.F. Froix, C.H. Griffiths, W. Gunning, A.J. Heeger, W.A. Little, J.S. Miller, M. Novatny, D.B. Tanner & M.L. Slade, *Ann. N. Y. Acad. Sci.* **313**, 459 (1978).

7. A.J. Epstein & J.S. Miller (to be published).

8. A.J. Epstein, E.M. Conwell, D.J. Sandman & J.S. Miller, *Solid State Commun.* **23**, 355 (1977).

9. A.J. Epstein & E.M. Conwell, *Solid State Commun.* **24**, 627 (1977).

10. A.J. Epstein, J.S. Miller & E.M. Conwell, *Ann. N. Y. Acad. Sci.* **313**, 183 (1978).

11. A. Brau, P. Brüesch, J.P. Farges, W. Hinz & D. Kuse, *Phys. Status Solidi (b)* **62**, 615 (1974).

12. D.B. Tanner, C.S. Jacobsen, A.A. Bright & A.J. Heeger, *Phys. Rev.* **B16**, 3283 (1977).

13. C.S. Jacobsen, D.B. Tanner, A.F. Garito & A.J. Heeger, *Phys. Rev. Lett.* **33**, 1559 (1974).

14. D.B. Tanner, C.S. Jacobsen, A.F. Garito & A.J. Heeger, *Phys. Rev.* **B13**, 3381 (1976).

15. J.B. Torrance, B.A. Scott & F.B. Kaufmann, *Solid State Commun.* **17**, 1369 (1975).

16. M.J. Rice, L. Pietronero & P. Bruesch, *Solid State Commun.* **21**, 757 (1977).

17. M.J. Rice, N.O. Lipari & S. Strassler, *Phys. Rev. Lett.* **39**, 1359 (1977).